ORAL DISEASES

Oral Diseases (2011) 17, 45–52. doi:10.1111/j.1601-0825.2010.01700.x

www.wiley.com

ORIGINAL ARTICLE

Improved visualization of low abundance oral fluid proteins after triple depletion of alpha amylase, albumin and IgG

G Krief[1*], O Deutsch[1*], S Gariba[1], B Zaks[1], DJ Aframian[2], A Palmon[1]

[1]*Hadassah Faculty of Dental Medicine, Institute of Dental Sciences, the Hebrew University, Jerusalem, Israel;* [2]*Salivary Gland Clinic, Saliva Diagnostic Laboratory, Hadassah Medical Center, Department of Oral Medicine, Hebrew University, Jerusalem, Israel*

OBJECTIVES: The aim of this study was to examine whether triple depletion of salivary-α-amylase (sAA), albumin (Alb) and immunoglobulins G (IgGs) may improve the visualization capability of proteins in two-dimensional gel electrophoresis (2-DE) of oral fluids (OF).

SUBJECTS AND METHODS: Oral fluids from healthy volunteers were subjected sequentially to sAA removing device followed by application to an Alb and IgG immunoaffinity column (triple depletion). The depleted OF samples were analyzed using SDS-PAGE followed by 2-DE and protein identification using ion-trap mass spectrometry (MS).

RESULTS: This specific triple depletion technique unmasked spots never visualized before. A total of 36 new spots were observed after depletion (348 *vs* 312 before depletion). Moreover, 58 spots showed more than twofold increase intensity after depletion. In the 60–69 kDa area, the depletion procedure unmasked 14 proteins including HSP70, LTA4H, L-Plastin, Desmoplakin that are known to be involved in disease pathogenesis.

CONCLUSION: The ability to selectively remove and elute the most abundant OF proteins visualized on the 2-DE represents an important step in the characterization of human OF. The better visualization and gel resolution achieved will improve quantification abilities in 2-DE and in tag-MS leading to better identification of disease-specific biomarkers. We further analyzed the eluted Alb and IgGs isoforms suggesting a new methodology venue for OF.

Oral Diseases (2011) **17**, 45–52

Keywords: Oral fluids; saliva biomarkers; amylase; albumin; immunoglobulin G; two-dimensional gel electrophoresis

Correspondence: Aaron Palmon, DMD, PhD, Institute of Dental Sciences, Faculty of Dental Medicine, The Hebrew University, Jerusalem, Israel. Tel/Fax: 972-2-6757595, E-mail: apalmon@cc.huji.ac.il

*Equally contributed to this study.

Received 5 January 2010; revised 4 March 2010; accepted 11 March 2010

Introduction

Oral fluids (OF) is a complex mixture of major and minor salivary gland secretions (saliva), gingival crevicular fluid, cell debris, microorganisms as well as bronchoalveolar and nasal secretions. Technological advances over the past decades have enabled the expansion of the utilization of OF in diagnosing disease-specific biomarkers, predicting disease progression, monitoring therapeutic drug levels and detecting illicit drug abuse. The easy non-invasive, user-friendly nature of its collection makes OF a valuable and powerful diagnostic clinical tool for defining the onset, progression and prognosis of human systemic diseases and in particular oral autoimmune and cancer diseases (Choo and Huestis, 2004; Ryu *et al*, 2006; Giusti *et al*, 2007; Hu *et al*, 2007a; Peluso *et al*, 2007; Streckfus and Dubinsky, 2007; Fleissig *et al*, 2009).

Recently, a consortium of three research groups has led to the identification of over 1166 saliva proteins (Denny *et al*, 2008). Most of the proteins were identified by shot gun proteomics, while in 2-DE pH 3 to pH 10 only ~300 proteins were visible as a result of the masking effect of high abundant proteins in the 2-DE maps (Hu *et al*, 2005). It is widely recognized that the protein profile of OF on 2-DE maps is dominated by a subset of abundant proteins mainly salivary-α-amylase (sAA) (Vitorino *et al*, 2004; Hu *et al*, 2005, 2007b, 2008; Oppenheim *et al*, 2007), Alb (Hu *et al*, 2005) and Immunoglobulins (Hu *et al*, 2005, 2007a; Hu *et al*, 2008; Kuhn *et al*, 2004) that mask potential low abundance biomarkers. Such masking, most probably, will also affect shot-gun proteomics as the overwhelming presence of numerous peptides derived from predominant proteins cause significant ion suppression when pursuing an analyte of interest (Kuhn *et al*, 2004). Changes in the OF representation of such high abundant proteins may be indicative of tissue damage but rarely provide a specific marker of disease. On the other hand, lower abundance proteins, present at the pictograms level, may offer markers for clinical diagnostics but require sensitive detection tools.

As a result of the heterogeneous nature of pathological course of disorders, it has been suggested that no single marker is likely to be sufficient for the prediction of a disease state and a panel of biomarkers should be exposed. This could be achieved by utilizing proteomic approaches on OF samples that have the capacity of profiling multiple biomarkers (Yao *et al*, 2003; Hu *et al*, 2005). Based on the successful compilation of the OF proteome, the next logical step would be to identify potential diagnostic biomarkers for clinical use. For this purpose technologies that enable protein visualization and quantification represent an advantage over other non-quantifying methodologies.

To utilize 2-DE proteomics or other high sensitivity quantifying methodologies for the purpose of identifying diagnostic biomarkers, it is crucial to develop new technologies to remove these proteins. In a previous study, we presented a new methodology for efficient, rapid and easy removal of sAA from OF using an affinity column (Deutsch *et al*, 2008). The aims of the current study were to examine if serum Alb, and IgGs depletion techniques could be modified for OF use, if further intervention using Alb, and IgGs depletion techniques may improve the visualization capability of proteins in 2-DE of OF and if these could be combined with sAA depletion methodology.

Materials and methods

OF collection
The complete OF accumulation protocol was approved by the Ethics Committee of Hadassah Medical Center, Jerusalem, Israel. Oral fluids (Unstimulated whole saliva) was collected from four age-matched healthy male volunteers (29.5 ± 1.8) into a precalibrated tube using the spitting method as previously described (Aframian *et al*, 2006).

Alb and IgGs removal capturing and elution
Two kits for Alb depletion methods in the serum were examined on OF and OF depleted from *sAA*; the SwellGel® Blue (PIERCE, Rockford, IL, USA) kit based on chemical interactions, and the ProteoPrep™ Immunoaffinity Albumin and IgG Depletion Kit (Sigma-Aldrich, St Louis, MO, USA) based on an immunoaffinity column. Alb and IgGs were removed from the OF using ProteoPrep® kit based on two antibodies immobilized in a matrix in a spin column. The protocol was changed for efficient removal from OF as follows: 500 μl of the OF sample was diluted with 125 μl of equilibration buffer and was loaded into the Alb and IgGs immunoaffinity spin column. The sample was incubated for 10 min and then was centrifuged for 1 min at 8000 *g*. The filtrate was collected and reloaded into the spin column for a second incubation to achieve maximum removal. After 10 min of the second incubation, the spin column was centrifuged for 1 min, 8000 *g*. To release unbinding proteins, 75 μl of equilibration buffer was added and centrifuged for 1 min 8000 *g*.

The procedure with the SwellGel® Blue kit was also changed for efficient removal from the OF as follows: one disk of the resin was hydrated in a spin column with 380 ml of ultrapure water. The column was centrifuged for 20 s at 12 000 *g* to remove the water. A 500 μl of OF sample, which was cleaned from salts, was then loaded into the column and incubated for 2 min. After the first incubation, the column was centrifuged for 1 min at 12 000 *g*. The filtrate was collected and reloaded back into the column for a second incubation of 20 min. This procedure was repeated twice to achieve an optimal removal of the Alb.

The captured Alb and IgGs were extracted from the spin column. The column was initially washed with 400 μl equilibration buffer to release unbinding proteins. To extract the Alb and IgGs, 150 μl of elution solution was added to the column and centrifuged for 1 min 8000 *g*. We repeated this step once more.

sAA affinity removal capturing and elution
Collected OF were subjected to the amylase removing device as previously described (Deutsch *et al*, 2008). After filtrating OF, which resulted in amylase–starch complexes, amylase was eluted from the potato starch matrix. The column with the starch was washed by slow hand pressed (30 s) with 1 ml elution buffer (995 μl of double distilled water (DDW) and 5 μl HCl, at 4°C). The eluted solution was titrated with NaOH up to the point of pH 6.5–8.5 and was dialyzed over night to remove the salts from the solution.

Protein concentration determination
Protein concentration was determined using the Bio-Rad Bradford protein assay (Bio-Rad, Hercules, CA, USA) as previously described (Bradford, 1976).

SDS-PAGE and 2-DE
Samples of 10 μg protein each of OF, OF depleted of Alb and IgGs, OF depleted of sAA, OF depleted of sAA and Alb and IgGs, the elution of sAA and Alb and IgGs were run on an 8% acrylamide mini gel, as previously described (Deutsch *et al*, 2008).

For analytical gels, samples of 45 μg proteins were subjected to rehydration followed by isoelectrofocusing in 18 cm long, pH 3–10 NL as previously described (Deutsch *et al*, 2008).

Imaging and statistical analysis
Gels were scanned using a computer GS-800 calibrated densitometer (Bio-Rad) and spots were detected and quantified using PDQuest software V 6.2.0 (Bio-Rad). Several limitations exist in 2D gel analysis as a result of gel to gel variation, and also because of the variability in the staining method. To overcome these drawbacks, all of the sample gels went through the same conditions simultaneously for the first and second dimensions. Normalization using PDQuest was performed by total density in image method to semi-quantify spot intensities and to minimize staining variation between gels.

MS identification
For MS identification, a 2-DE containing 100 μg protein sample was prepared and fixed in 50% (v/v) ethanol,

12% (v/v) acetic acid for 2 h. Proteins were visualized by staining with a SilverQuest staining kit for MS compatible silver staining (SilverQuest, Invitrogen, Carlsbad, CA, USA). Electrophoretically separated spots were sterilely excised from gels, and in-gel reduced (10 mM Dithiothreitol, incubated at 60°C for 30 min), alkylated (10 mM iodoacetamide, at room temperature for 30 min) and proteolyzed with trypsin (overnight at 37°C using modified trypsin, Promega) at a 1:100 enzyme-to-substrate ratio) according to Wilton *et al*, 1989.

The resulting tryptic peptides were resolved by reversed-phase chromatography on 0.1 × 200-mm fused silica capillaries (J&W, 100 micrometer ID) packed with Everest reversed phase material (Grace Vydac, Hesperia, CA, USA). The peptides were eluted with a 45 min gradient of 5 to 95% (v/v) of acetonitrile with 0.1% (v/v) formic acid in water at flow rates of 0.4 μl min^{-1}. Mass spectrometry was performed by an ion-trap MS (Orbitrap; Thermo, Rockford, IL, USA) in a positive mode using a repetitively full MS scan followed by collision induced dissociation (CID) of the five most dominant ion selected from the first MS scan.

The MS data were clustered and analyzed using Sequest software (version 3.31; J. Eng and J. Yates, University of Washington and Finnigan, San Jose, USA) and Pep-Miner (Beer *et al*, 2004) searching against the human part of the Uniprot database. The results were filtered according to the Xcorr value (1.5 for singly charged peptides, 2.2 for doubly charged peptides and 3 for triply charged peptides).

Results

SDS-PAGE and densitometry analysis of depleted OF

Figure 1 shows OF and OF depleted of Alb after treatment with SwellGel® Blue (lane 2) or with ProteoPrep™ (lane 3) after SDS-PAGE separation. Quantity analysis of the 69 kDa band, corresponding to Alb, by optical density, showed a threefold reduction in the ProteoPrep™ treated sample ($n = 4$, $P < 0.05$), while only a 1.6 fold reduction was revealed in the SwellGel® Blue treated sample ($n = 4$, $P < 0.05$). Therefore, for further depletion analysis the ProteoPrep™ kit was utilized.

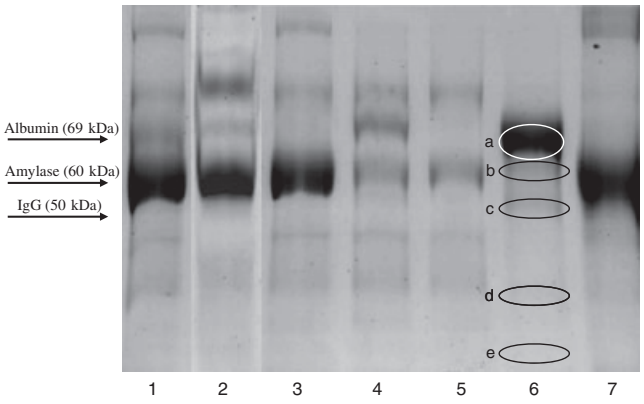

Figure 1 SDS-PAGE of depleted oral fluid (OF) and elution. A 10 μg of human OF proteins was separated on an 8% acrylamide-gel and stained with Coomassie-Brilliant-Blue. OF (1), Alb depleted with ProteoPrep® (Sigma-Aldrich, USA) (2), salivary-α-amylase (sAA) depleted (3), sAA and Alb depleted (4), Alb elution (5) sAA elution (6), Alb depleted with SwellGel® Blue (PIERCE, USA) (7). Bands a–e (5) were identified using Mass spectrometry, showing mainly Alb and immunoglobulin derivatives

Figure 1 demonstrates the removal of Alb and IgGs treated by ProteoPrep™ (lane 3), the removal of sAA by means of the amylase removing device (lane 4) and the combination of these two methods (lane 5). The bands in the 60 kDa and 69 kDa area after depletion suggest new protein components that were masked by sAA and Alb. To test the specificity of the removal methodology, Figure 1 (lane 6) shows Alb and IgGs elution from the kit and lane 7 represents sAA after elution from the device. Salivary-α-amylase elution was specific as we reported before (Deutsch *et al*, 2008). Mass spectrometry analysis of the bands in the Alb and IgGs elution sample identified that 92% of the matched peptides from the elution sample were Alb or IgGs derivatives. These results directly indicate the specific removal of Alb and IgGs from OF as the majority of the proteins which were detected using MS were Alb and IgGs.

2-DE and MS analysis after triple depletion

Figure 2a (lower panel) shows the 2-DE gel of OF and Figure 2b (lower panel) shows the same OF sample after depletion. Analysis of the 2-DE silver-stained gel revealed a similar protein pattern with the exception of the 60 and 69 kDa areas corresponding to sAA and Alb, respectively. Excluding sAA and Alb area, 312 spots were observed before depletion while 348 spots detected after depletion. Moreover, 58 spots had more than twofold increase intensity after depletion. Figure 2b (lower panel) shows 22 (of 36) new major spots all over the gel (dashed circles). Major areas with different protein profile expressions are demonstrated as a direct result of the depletion treatment. Two dashed black ellipses indicate spots of low abundant proteins with increased intensity after depletion. On the contrary, two dashed black rectangles indicate major sAA, Alb and IgGs areas and therefore decrease the triple after depletion process.

A semi-quantitative analysis of the 2-DE images before and after protein removal indicates that the densitometry intensity of the Alb area (Figure 2 -upper panels, white dashed ellipse, 69 kDa area) normalized by the total volume of the spots was reduced from ~9.0%, before depletion, to ~1.2%, after depletion corresponding to 87% reduction. In addition, a semi-quantitative analysis of the major IgGs area (Figure 2 upper panels white dashed rectangle, 50 kDa area) showed ~94% reduction after treatment.

A difference in 1-DE and 2-DE densitometry analyses (70% and 87% reduction, respectively) was observed. This observation could be explained by the fact that 2-DE enables a more accurate analysis of the Alb area while 1-DE enables only an analysis of the entire 69 kDa area which includes proteins in addition to Alb as well.

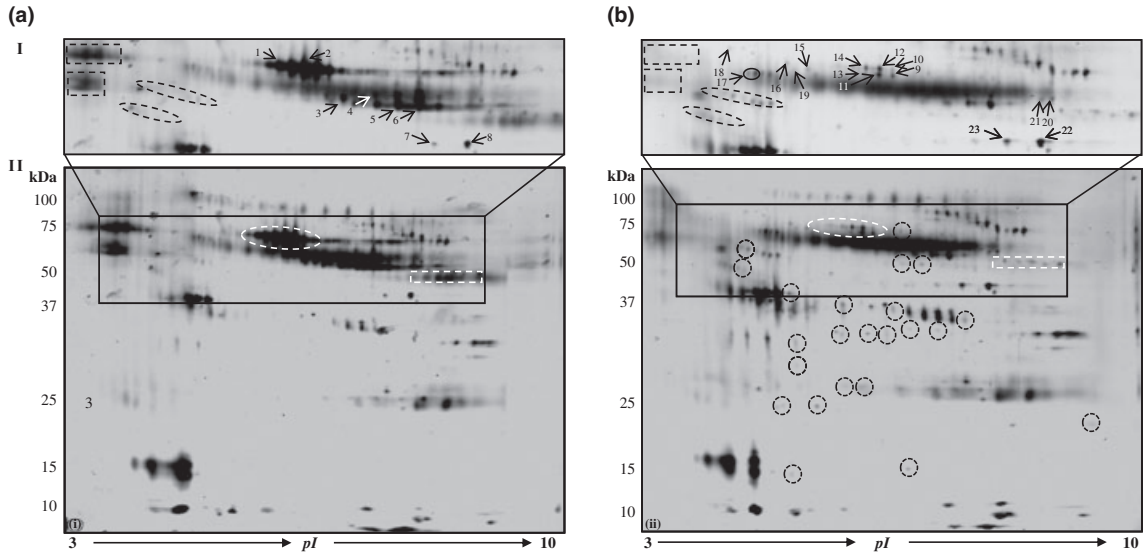

Figure 2 Silver stained 2-DE analysis (45 μg) of oral fluid (OF) (**a**) and triple-depleted-OF (**b**). Lower panels (II) show complete gel. Black rectangle indicates major salivary-α-amylase (sAA) area, dashed-white-ellipse indicates Alb area and dashed-white-rectangle indicates IgGs areas. Upper panels (I) show magnification of sAA, Alb & IgGs major areas illustrating the effectiveness of the depletion. Dashed-black-circles indicate major new proteins revealed after depletion. Spots identified are numbered

Unmasking effect

To demonstrate the unmasking effect of the combined depletion process, we focused on the sAA and Alb area. Figure 2a (upper panels) show magnification of the identified sAAs, Alb and IgGs major areas which is in agreement with the previous reports (Hirtz *et al*, 2005; Hu *et al*, 2005, 2007a; Kuhn *et al*, 2004). A series of spots (#1 to #8) from OF gel before depletion were identified using MS and served to match the other spots (#9–23, taken from the depleted gel) with previously reported maps (Yao *et al*, 2003; Hirtz *et al*, 2005; Hu *et al*, 2005; Deutsch *et al*, 2008). Most of the spots identified (#1 to #6) were sAAs, Alb and IgGs (Table 1). Spots #7–8 and spots #22–23 from the depleted gel served as anchoring points between gels.

In the previous study, we focused on the sAA (60 kDa) area only and revealed 13 spots which contained 15 proteins after sAA depletion (Deutsch *et al*, 2008). In the current study in the depleted OF gel (Figure 2b, upper panel), additional 13 spots (#9 to #21) were excised and subsequently identified using MS. Table 1 represents the identities of the spots after depletion. Spot numbers #9 to #14 were masked by Alb before depletion. To focus on the main data, proteins which were MS identified with four or less peptides were excluded (mainly keratins, based on the assumption that reduced matched peptide numbers usually indicate lower protein content, for review see Bantscheff *et al*, 2007). Four new proteins that were not visualized before in this area were exposed. Spots #9 to #14 also contained some remnants of serum Alb precursor. Spot numbers #15 to #21 demonstrate low abundant proteins in which their spot intensity increased as a result of the depletion treatment. These spots revealed 10 proteins that most of them were not visualized in the 2-DE before the depletion treatment.

OF SDS-PAGE, 2-DE and MS analysis of Alb and IgGs elution

To characterize the expression profile of the different Alb and IgGs proteins isoforms, we performed a 2-DE of the eluted solution. A semi-quantitative densitometric analysis indicated that the level of Alb area (Figure 3, white dashed ellipse) normalized by the total proteins spots volume corresponded to threefold increase from ~9.0%, in OF, to ~31%, after elution. In addition, a semi-quantitative analysis of major IgGs area (Figure 3 white dashed rectangle, 50 kDa area), revealed ~3.4 fold increase.

As a result of the restricted variety of proteins in the elution sample, 2-DE suggest a unique pattern composed of 10 clusters which include mainly Alb and IgGs and almost no isolated spots in comparison with 2-DE of OF.

From 17 spots that were analyzed using MS, 34 different proteins were identified (Table 2). As the elution proteomics map was never analyzed before we excluded only proteins with less than two matched peptides.

Discussion

High abundant protein depletion possesses two possible effects: (i) It increases gel resolution by raising the relative portion of the low abundant proteins in the proteomic map and (ii) It unmasks low abundant proteins which may serve as possible biomarkers by removing overlapping high abundant spots. Both of these effects are demonstrated in the triple depletion gel presented in this study.

In our previous study describing a new methodology to remove sAA which serves as the most abundant protein in OF, we still could visualize other protein masking components existing in OF, mainly, Albs and

Table 1 A list of proteins identified in the high-abundant salivary-α-amylase, Alb & IgGs area, before (spots #1–8) and after triple depletion (spots #9–23)

Spot	*Protein identification*	*Accession no.*	*Theor. MW (Da)*	*Theor. pI*	*Matched peptides*	*Sequence coverage (%)*
1	Serum albumin precursor	P02768	69180	5.91	22	30
2	Serum albumin precursor	P02768	69180	5.91	20	31
3–6	Salivary α-amylase	P04745	57768	6.47	–	–
7, 22	α-enolase	P06733	47139	7.01	15	46
8, 23	α-enolase	P06733	47139	7.01	9	35
9	Leukotriene A-4 hydrolase	P09960	69241	5.80	20	27
	Desmoplakin	P15924	331568	6.44	14	5
	Serum albumin precursor	P02768	69322	5.92	10	13
	Ig alpha-1 chain C region	P01876	37631	6.08	9	26
	Keratin, type I cytoskeletal 16	P08779	51236	4.98	7	15
10	Serum albumin precursor	P02768	69322	5.92	11	18
11	Leukotriene A-4 hydrolase	P09960	69241	5.80	19	31
	Ig alpha-1 chain C region	P01876	37631	6.08	8	24
	Desmoplakin	P15924	331568	6.44	7	2
12	Serum albumin precursor	P02768	69322	5.92	14	22
	Leukotriene A-4 hydrolase	P09960	69241	5.80	6	11
13	Leukotriene A-4 hydrolase	P09960	69241	5.80	8	16
	Serum albumin precursor	P02768	69322	5.92	8	12
14	Serum albumin precursor	P02768	69322	5.92	14	19
15	Serum albumin precursor	P02768	69322	5.92	14	30
	Heat shock 70 kDa protein 1L	P34931	70331	5.76	9	13
	Heat shock 70 kDa protein 1	P08107	70009	5.48	8	11
16	Heat shock cognate 71 kDa protein	P11142	70854	5.37	6	9
	Heat shock 70 kDa protein 1L	P34931	70331	5.76	6	9
17	Plastin-2	P13796	70245	5.20	28	31
	Ig alpha-1 chain C region	P01876	37631	6.08	9	25
18	78 kDa glucose-regulated protein precursor	P11021	72289	5.07	18	29
	Dipeptidyl-peptidase 3	Q9NY33	82538	5.01	6	8
19	Keratin, type II cytoskeletal 1b	Q7Z794	61650	5.63	7	13
	Heat shock cognate 71 kDa protein	P11142	70854	5.37	7	9
	Ig alpha-1 chain C region	P01876	37630.65	6.08	6	20
20	Catalase	P04040	59719	6.90	15	29
	Keratin, type I cytoskeletal 16	P08779	51236	4.98	7	18
21	Catalase	P04040	59719	6.90	18	33
	Ig alpha-1 chain C region	P01876	37631	6.08	8	24

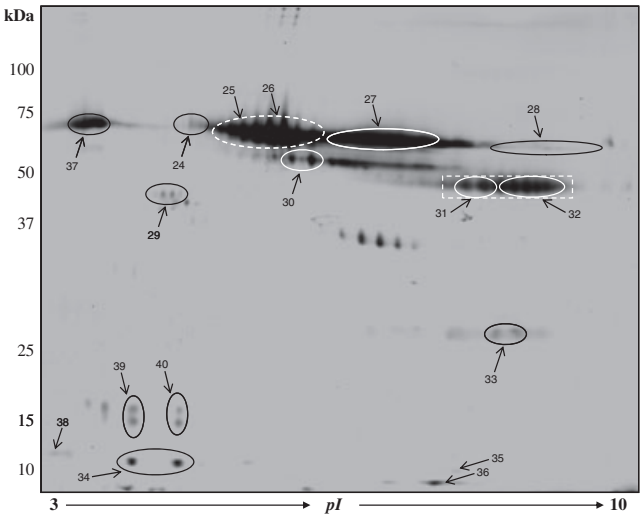

Figure 3 Silver stained 2-DE analysis (45 μg) of albumin and IgGs isoforms. Dashed white ellipse and rectangle indicate major albumin and immunoglobulin areas, respectively. Spots identified by Mass Spectrometry are numbered

IgGs (Deutsch *et al*, 2008). These findings were also supported in other 2-DE studies (Hu *et al*, 2007b; Hu *et al*, 2005, 2007a; Hu *et al*, 2008).

In addition to the 13 spots identified before by sAA depletion only, 14 proteins, which were previously undetectable, were revealed in the 60–69 kDa area after the triple depletion procedure. The low abundant proteins revealed may serve in the future as possible biomarkers for severe oral and systemic diseases, for instance, heat shock protein 70 (HSP70, Accession no.: P34931, spots #15, #16) has been reported to be involved in inhibition of apoptosis processes in several types of cancers such as oral, breast and pancreatic cancers (Aghdassi *et al*, 2007; Kaur and Ralhan, 2000; Sherman and Multhoff, 2007). Moreover, HSP70 has been suggested as a potential therapeutic regiment for pancreatic and oral cancer (Saluja and Dudeja, 2008; Markopoulos *et al*, 2009). Interestingly, HSP70 has also been reported to be involved in Alzheimer's disease pathogenesis (Koren *et al*, 2009).

Leukotriene A4 Hydrolase (LTA4H, Accession no.: P09960, spots #9, #11 to #13) is a bifunctional zinc enzyme with the activities of epoxide hydrolase and aminopeptidase. As an epoxide hydrolase, LTA4H catalyzes the hydrolysis of the epoxide LTA4 to the diol, leukotriene B4 (LTB4), which mainly functions as a chemo-attractant and an activator of inflammatory cells (Chen *et al*, 2004) and known to increase significantly in

Table 2 A list of proteins identified from 2-DE of Alb & IgGs elution

Spot	*Protein identification*	*Accession no.*	*Theor. MW (Da)*	*Theor. pI*	*Matched peptides*	*Sequence coverage (%)*
24	Serum albumin precursor	P02768	69322	5.92	30	39
	Desmoplakin	P15924	331568	6.44	13	5
	Junction plakoglobin	P14923	81578	5.75	5	7
	Keratin, type I cytoskeletal 16	P08779	51236	4.98	4	13
	Keratin, type I cytoskeletal 13	P13646	49555	4.91	4	8
	Keratin, type II cytoskeletal 1b	Q7Z794	61650	5.63	4	7
	Ig alpha-1 chain C region	P01876	37631	6.08	3	10
	Alpha-amylase 1 precursor	P04745	57731	6.47	3	7
	Extracellular glycoprotein lacritin precursor	Q9GZZ8	14237	5.44	2	17
	Peroxiredoxin-1	Q06830	22096	8.27	2	10
	Arginase-1	P05089	34713	6.72	2	7
	Serpin B12	Q96P63	46247	5.36	2	6
	Desmocollin-1 precursor	Q08554	99982	5.25	2	3
25	Serum albumin precursor	P02768	69322	5.92	38	55
	Ig alpha-1 chain C region	P01876	37631	6.08	5	16
	Keratin, type I cytoskeletal 13	P13646	49555	4.91	2	5
26	Serum albumin precursor	P02768	69322	5.92	42	61
	Keratin, type I cytoskeletal 16	P08779	51236	4.98	7	21
	Ig alpha-1 chain C region	P01876	37631	6.08	6	18
	Protein-glutamine gamma-glutamyltransferase E precursor	Q08188	76710	5.81	3	5
27	Keratin, type I cytoskeletal 16	P08779	51236	4.98	4	13
	Bactericidal/permeability-increasing protein-like 1 precursor	Q8N4F0	49142	8.48	2	5
	Keratin, type I cytoskeletal 13	P13646	49555	4.91	2	5
	Junction plakoglobin	P14923	81578	5.75	2	3
28	Serum albumin precursor	P02768	69322	5.92	22	30
	Keratin, type I cytoskeletal 13	P13646	49555	4.91	4	9
	Keratin, type I cytoskeletal 16	P08779	51236	4.98	3	7
	Ig gamma-1 chain C region	P01857	36083	8.46	2	5
29	Keratin, type I cytoskeletal 16	P08779	51236	4.98	6	13
	Keratin, type I cytoskeletal 13	P13646	49555	4.91	4	9
	Serum albumin precursor	P02768	69322	5.92	3	4
	Keratin, type II cytoskeletal 1b	Q7Z794	61650	5.63	2	4
	Desmoplakin	P15924	331568	6.44	2	1
30	Serum albumin precursor	P02768	69322	5.92	26	33
	Ig alpha-1 chain C region	P01876	37631	6.08	6	18
	Keratin, type I cytoskeletal 16	P08779	51236	4.98	2	7
	Keratin, type I cytoskeletal 17	Q04695	48076	4.97	2	5
	Keratin, type I cytoskeletal 13	P13646	49555	4.91	2	5
31	Keratin, type I cytoskeletal 13	P13646	49555	4.91	8	16
	Ig gamma-1 chain C region	P01857	36083	8.46	7	22
	Serum albumin precursor	P02768	69322	5.92	4	7
	Ig heavy chain V-III region GAL	P01781	12722	8.7	2	23
	Ig heavy chain V-III region VH26 precursor	P01764	12574	8.49	2	19
	Ig gamma-2 chain C region	P01859	35862	7.66	2	8
	Bactericidal/permeability-increasing protein-like 1 precursor	Q8N4F0	49142	8.48	2	5
	Keratin, type II cytoskeletal 3	P12035	64465	6.12	2	3
32	Ig gamma-1 chain C region	P01857	36083	8.46	10	24
	Keratin, type I cytoskeletal 13	P13646	49555	4.91	6	12
	Keratin, type I cuticular Ha1	Q15323	47202	4.84	4	11
	Keratin type II cuticular Hb1	Q14533	54936	5.48	4	8
	Serum albumin precursor	P02768	69322	5.92	4	6
	Keratin, type I cytoskeletal 17	Q04695	48076	4.97	3	7
	Desmoplakin	P15924	331568	6.44	3	1
	Ig heavy chain V-III region WEA	P01763	12249	8.7	2	26
	Ig heavy chain V-III region VH26 precursor	P01764	12574	8.49	2	19
	Ig gamma-2 chain C region	P01859	35862	7.66	2	8
	Keratin type II cuticular Hb2	Q9NSB4	56616	6.4	2	4
	Keratin, type II cytoskeletal 3	P12035	64465	6.12	2	2
33	Serum albumin precursor	P02768	69322	5.92	5	9
	Ig kappa chain C region	P01834	11602	5.58	4	55
	Ig kappa chain V-I region CAR	P01596	11696	9.47	3	17
	Ig kappa chain V-I region Ni	P01613	12238	5.25	3	16
	Ig kappa chain V-III region SIE	P01620	11768	8.7	2	25
	Ig lambda chain V-III region LOI	P80748	11928	4.94	2	22
	Ig kappa chain V-I region AG	P01593	11985	5.67	2	17
	Ig kappa chain V-I region Wes	P01611	11601	6.91	2	17
	Ig kappa chain V-I region DEE	P01597	11654	9.43	2	17

Table 2 (Continued)

Spot	*Protein identification*	*Accession no.*	*Theor. MW (Da)*	*Theor. pI*	*Matched peptides*	*Sequence coverage (%)*
34	Prolactin-inducible protein precursor	P12273	16562	8.26	3	23
	Serum albumin precursor	P02768	69322	5.92	3	4
35	Ig gamma-1 chain C region	P01857	36083	8.46	2	6
	Keratin, type I cytoskeletal 17	Q04695	48076	4.97	2	5
	Keratin, type I cytoskeletal 13	P13646	49555	4.91	2	5
36	Keratin, type I cytoskeletal 16	P08779	51236	4.98	5	11
	Ig gamma-1 chain C region	P01857	36083	8.46	2	6
	Keratin, type I cytoskeletal 17	Q04695	48076	4.97	2	5
	Keratin, type I cytoskeletal 13	P13646	49555	4.91	2	5
37	Serum albumin precursor	P02768	69322	5.92	8	14
	Keratin, type I cytoskeletal 13	P13646	49555	4.91	2	5
38	Ig alpha-1 chain C region	P01876	37631	6.08	3	12
	Keratin, type I cytoskeletal 16	P08779	51236	4.98	3	7
	Keratin, type I cytoskeletal 13	P13646	49555	4.91	2	5
39	Prolactin-inducible protein precursor	P12273	16562	8.26	3	26
	Lipocalin-1 precursor	P31025	19238	5.39	2	11
	Ig alpha-1 chain C region	P01876	37631	6.08	2	9
40	Desmoplakin – *Homo sapiens* (Human)	P15924	331568	6.44	19	7
	Junction plakoglobin	P14923	81578	5.75	7	10
	Keratin, type I cytoskeletal 16	P08779	51236	4.98	6	14
	Prolactin-inducible protein precursor	P12273	16562	8.26	3	23
	Desmoglein-1 precursor	Q02413	113644	4.9	3	3
	Arginase-1	P05089	34713	6.72	2	7
	Annexin A2	P07355	38580	7.57	2	6
	Keratin, type I cytoskeletal 17	Q04695	48076	4.97	2	5
	Keratin, type I cytoskeletal 13	P13646	49555	4.91	2	5

human atherosclerotic plaque (Qiu *et al*, 2006). In addition, its over expression appears to be an early event in esophageal adenocarcinogenesis and was suggested as a potential target for the chemoprevention of esophageal adenocarcinogenesis (Chen *et al*, 2003, 2004).

Another low abundant protein reveled by the triple depletion techniques was L-Plastin (Accession no.: P13796, spots #15, #17) which is an actin binding protein expressed in the cells of the haematopoetic lineage. L-Plastin was reported to be down regulated in several cancers (Samstag and Klemke, 2007). Finally, a pivotal protein with increased matched peptide number was Desmoplakin. Desmoplakin, a desmosomal component, is a key protein involved in cell–cell adhesion. (Presland and Dale, 2000; Papagerakis *et al*, 2009). Down-regulation of desmosomal proteins is associated with the invasive and metastatic ability of tumor cells and was suggested for evaluation risk of distant metastasis formation in oral cancer patients (Papagerakis *et al*, 2009). In addition, it was reported recently to be down-regulated in saliva among type II diabetes patients (Rao *et al*, 2009).

Elution of the albumin and IgGs from the immunoaffinity demonstrated the variety of isoforms and therefore, suggests that analysis of these captured proteins and their expression patterns might be useful in searching and characterizing new disease bio-markers.

In conclusion, this study represents an important step in the characterization of human OF. The ability to selectively remove and elute the most abundant OF proteins visualized on the 2-DE map, namely, sAA, Alb and IgGs revealed unmasked non-visualized spots and increased gel resolution, mainly in the 60–69 kDa area. The better resolution and higher protein amounts subjected to 2-DE proteomic analysis increases the potential of discovery novel biomarkers and consequently contribute to the effort of defining OF biomarkers for detection of diseases as well as for monitoring their progression.

Acknowledgement

This research was supported by THE ISRAEL SCIENCE FOUNDATION (no. 802/05) and by AFHU. MS identification by Smoler Proteomics Center at the Technion.

References

Aframian DJ, Davidowitz T, Benoliel R (2006). The distribution of oral mucosal pH values in healthy saliva secretors. *Oral Dis* **12:** 420–423.

Aghdassi A, Phillips P, Dudeja V *et al* (2007). Heat shock protein 70 increases tumorigenicity and inhibits apoptosis in pancreatic adenocarcinoma. *Cancer Res* **67:** 616–625.

Bantscheff M, Schirle M, Sweetman G, Rick J, Kuster B (2007). Quantitative mass spectrometry in proteomics: a critical review. *Anal Bioanal Chem* **389:** 1017–1031.

Beer I, Barnea E, Ziv T, Admon A (2004). Improving large-scale proteomics by clustering of mass spectrometry data. *Proteomics* **4:** 950–960.

Bradford MN (1976). A rapid and sensitive method for the quantitation of microgram quantities of protein utilizing the principle of protein-dye binding. *Anal Biochem* **72:** 248–254.

Chen X, Li N, Wang S *et al* (2003). Leukotriene A4 hydrolase in rat and human esophageal adenocarcinomas and inhibitory effects of bestatin. *J Natl Cancer Inst* **16:** 1053–1061.

Chen X, Wang S, Wu N, Yang CS (2004). Leukotriene A4 hydrolase as a target for cancer prevention and therapy. *Curr Cancer Drug Targets* **4:** 267–283.

Choo RE, Huestis MA (2004). Oral fluid as a diagnostic tool. *Clin Chem Lab Med* **42:** 1273–1287.

Denny P, Hagen FK, Hardt M *et al* (2008). The proteomes of human parotid and submandibular/sublingual gland salivas collected as the ductal secretions. *J Proteome Res* **7:** 1994–2006.

Deutsch O, Fleissig Y, Zaks B, Krief G, Aframian DJ, Palmon A (2008). An approach to remove alpha amylase for proteomic analysis of low abundance biomarkers in human saliva. *Electrophoresis* **29:** 4150–4157.

Fleissig Y, Deutsch O, Reichenberg E *et al* (2009). Different proteomic protein patterns in saliva of Sjögren's syndrome patients. *Oral Dis* **15:** 61–68.

Giusti L, Baldini C, Bazzichi L *et al* (2007). Proteome analysis of whole saliva: a new tool for rheumatic diseases-the example of Sjögren's syndrome. *Proteomics* **7:** 1634–1643.

Hirtz C, Chevalier F, Centeno D *et al* (2005). MS characterization of multiple forms of alpha-amylase in human saliva. *Proteomics* **5:** 4597–4607.

Hu S, Xie Y, Ramachandran P *et al* (2005). Large-scale identification of proteins in human salivary proteome by liquid chromatography/mass spectrometry and two-dimensional gel electrophoresis-mass spectrometry. *Proteomics* **5:** 1714–1728.

Hu S, Yu T, Xie Y *et al* (2007a). Discovery of oral fluid biomarkers for human oral cancer by mass spectrometry. *Cancer Genomics Proteomics* **4:** 55–64.

Hu S, Loo JA, Wong DT (2007b). Human saliva proteome analysis. *Ann N Y Acad Sci* **1098:** 323–329.

Hu S, Arellano M, Boontheung P *et al* (2008). Salivary proteomics for oral cancer biomarker discovery. *Clin Cancer Res* **14:** 6246–6252.

Kaur J, Ralhan R (2000). Induction of apoptosis by abrogation of HSP70 expression in human oral cancer cells. *Int J Cancer* **85:** 1–5.

Koren J 3rd, Jinwal UK, Lee DC *et al* (2009). Chaperone signalling complexes in Alzheimer's disease. *J Cell Mol Med* **13:** 619–630.

Kuhn E, Wu J, Karl J, Liao H, Zolg W, Guild B (2004). Quantification of C-reactive protein in the serum of patients with rheumatoid arthritis using multiple reaction monitoring mass spectrometry and 13C-labeled peptide standards. *Proteomics* **4:** 1175–1186.

Markopoulos AK, Deligianni E, Antoniades DZ (2009). Heat shock protein 70 membrane expression in oral cancer: a possible new target in antineoplastic therapy? *Chemotherapy* **11:** 211–214.

Oppenheim FG, Salith E, Siqueira W, Zhang W, Helmerhorst EJ (2007). Salivary proteome and its genetic polymorphisms. *Ann N Y Acad Sci* **1098:** 22–50.

Papagerakis S, Shabana AH, Pollock BH, Papagerakis P, Depondt J, Berdal A (2009). Altered desmoplakin expression at transcriptional and protein levels provides prognostic information in human oropharyngeal cancer. *Hum Pathol* **40:** 1320–1329.

Peluso G, De Santis M, Inzitari R *et al* (2007). Proteomic study of salivary peptides and proteins in patients with Sjögren's syndrome before and after pilocarpine treatment. *Arthritis Rheum* **56:** 2216–2222.

Presland RB, Dale BA (2000). Epithelial structural proteins of the skin and oral cavity: function in health and disease. *Crit Rev Oral Biol Med* **11:** 383–408.

Qiu H, Gabrielsen A, Agardh HE *et al* (2006). Expression of 5-lipoxygenase and leukotriene A4 hydrolase in human atherosclerotic lesions correlates with symptoms of plaque instability. *Proc Natl Acad Sci USA* **103:** 8161–8166.

Rao PV, Reddy AP, Lu X *et al* (2009). Proteomic identification of salivary biomarkers of type-2 diabetes. *J Proteome Res* **8:** 239–245.

Ryu OH, Atkinson JC, Hoehn GT, Illei GG, Hart TC (2006). Identification of parotid salivary biomarkers in Sjogren's syndrome by surface-enhanced laser desorption/ionization time-of-flight mass spectrometry and two-dimensional difference gel electrophoresis. *Rheumatology* **45:** 1077–1086.

Saluja A, Dudeja V (2008). Heat shock proteins in pancreatic diseases. *J Gastroenterol Hepatol* **23:** S42–S45.

Samstag Y, Klemke M (2007). Ectopic expression of L-plastin in human tumor cells: diagnostic and therapeutic implications. *Adv Enzyme Regul* **47:** 118–126.

Sherman M, Multhoff G (2007). Heat shock proteins in cancer. *Ann N Y Acad Sci* **1113:** 192–201.

Streckfus CF, Dubinsky WP (2007). Proteomic analysis of saliva for cancer diagnosis. *Expert Rev Proteomics* **4:** 329–332.

Vitorino R, Lobo MJ, Ferrer-Correira AJ *et al* (2004). Identification of human whole saliva protein components using proteomics. *Proteomics* **4:** 1109–1115.

Wilton JM, Curtis MA, Gillett IR *et al* (1989). Detection of high-risk groups and individuals for periodontal diseases: laboratory markers from analysis of saliva. *J Clin Periodontol* **16:** 475–483.

Yao Y, Berg EA, Costello CE, Troxler RF, Oppenheim FG (2003). Identification of protein components in human acquired enamel pellicle and whole saliva using novel proteomics approaches. *J Biol Chem* **278:** 5300–5308.